

# 2D material manipulation in the electron microscope under low-pressure atmospheres

U. Javed<sup>1</sup>, B.M. Mayer<sup>1,2</sup>, E.H. Åhlgren<sup>1,2</sup>, M. Längle<sup>1,3</sup>, T. Susi<sup>1</sup>, Jani Kotakoski<sup>1\*</sup>

<sup>1</sup>University of Vienna, Boltzmanngasse 5, 1090 Vienna, Austria

<sup>2</sup>Uppsala University, Box 516, Uppsala SE-751 20, Sweden

<sup>3</sup>University Paris-Saclay, 510 Rue André Rivière, Paris, 91405, France

\*jani.kotakoski@univie.ac.at

It is well established that electron irradiation during (scanning) transmission electron microscopy imaging can influence the structure of the studied sample due to elastic and inelastic scattering [1]. While the first of these, which dominates for conductive materials, is fairly well understood, the role of excitations arising from inelastic scattering remains under active research [2–5]. At the same time, the equally important role of the residual vacuum in the microscope is often completely neglected. Indeed, [6,7], it has an influence already at fairly low pressures ( $10^{-7}$  mbar) on carbon structures without ideal  $sp^2$  bonding (hydrocarbon contamination, defects and pores in graphene) where the partial pressure of oxygen can even determine the observed termination of a graphene edge. In the case of more oxygen-sensitive materials such as  $\text{MoTe}_2$ , the presence of oxygen in the column significantly accelerates the beam-induced damage even for the pristine material [8], whereas structurally similar but chemically more inert  $\text{MoS}_2$  remains unaffected. As will be shown here, controlling residual oxygen partial pressure in the microscope allows also determining the shape of pores created into hBN during imaging, where pores created under ultra-high vacuum show no clear edge-termination preference, but under a low-pressure oxygen atmosphere nitrogen-terminated triangle-shaped pores are dominant [9]. Interestingly, similar experiments under a methane atmosphere lead to triangle-shaped pores with the opposite orientation, as well as to carbon-containing inclusions in the otherwise pristine material [10].

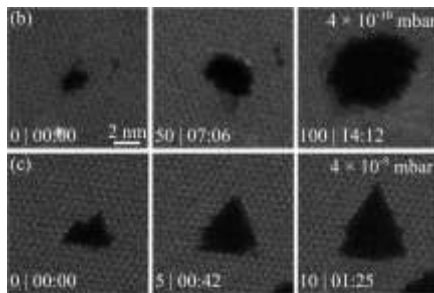


Fig. 1: Pores created into hBN during imaging in (top) ultra-high vacuum and (bottom) under  $\text{O}_2$ .

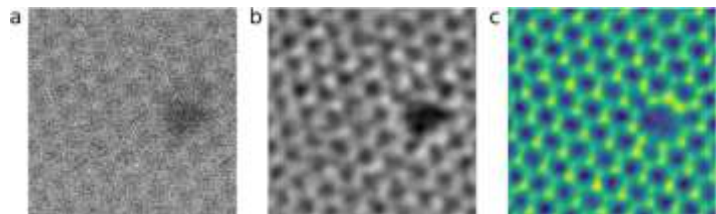


Fig. 2: A triangular pore created into hBN under a methane atmosphere. (a) HAADF, (b) filtered HAADF, and (c) single-sideband reconstruction images.

## References:

- [1] T. Susi et al., Nat. Rev. Phys. **1**, 397-405 (2019)
- [2] S. Kretschmer et al., Nano Lett. **20**, 2865 (2020)
- [3] T.A. Bui et al., Small **19**, 2301926 (2023)
- [4] C. Speckmann et al., Phys. Rev. B **107**, 094112 (2023)
- [5] A. Yoshimura et al, Nanoscale **15**, 1053 (2023)
- [6] G.T. Leuthner et al., Ultramicroscopy **203**, 76-81 (2019)
- [7] G.T. Leuthner et al., 2D Mater. **8**, 035023 (2021)
- [8] E.H. Åhlgren et al, Adv. Mater. Interfaces **9**, 2200987 (2022)
- [9] U. Javed et al, arXiv: 2507.13180 (2025)
- [10] B.M. Mayer et al., in preparation (2026)

# THE TEM: A VERSATILE TOOLKIT FOR EXPLORING QUANTUM MECHANICS

Stefan Löffler<sup>1\*</sup>

<sup>1</sup>TU Wien, USTEM, Stadionallee 2, 1020, Wien, Austria

\*stefan.loeffler@tuwien.ac.at

Traditionally, the transmission electron microscope (TEM) is often considered as a sample characterization tool for tasks such as imaging the sample, measuring atomic positions and determining atom types. However, this application-centered approach neglects that, on a fundamental level, the TEM in fact realizes an experimental setup for a quantum-mechanical scattering experiment: the condenser lens system prepares the probe electron's state according to the experimenters' specifications, then the probe electron interacts with the specimen, and finally the outgoing probe electron's state is measured (e.g., its spatial, momentum, or energy distribution).

In this presentation, I will explore some of the quantum mechanical phenomena that can occur in the different parts of the TEM. Before and after the sample area, one is free to manipulate the quantum state of the probe itself, e.g. using beam shaping to create specific states such as vortex beams [2]. On the one hand, this allows to directly study and experiment with electron states, such as free-electron Landau states [4]. On the other hand, this paves the way of transforming one state into another to optimize measurements [2,3].

Regarding the sample, one usually has no means of determining its local quantum state on a nanometer scale before or after the interaction with the beam electron (after all, gaining information about the sample is the very point of investigating it in the TEM). In effect, this means that we are dealing with the interaction between a specifically prepared quantum system (of the beam electron) with a largely undetermined quantum system (of the sample). On a practical level, I will review ways of determining properties of the quantum system of the sample, such as the spatial distribution or spin information of individual states [4,5]. On a more fundamental level, I will discuss the fact that the interaction between quantum systems gives rise to entanglement, which has been largely neglected thus far [6].

Both the probe beam and the sample are inherently quantum mechanical objects. Fully embracing that fact may not only provide new insights into the underlying physics governing them as well as their interaction, it can also pave the way for new, optimized measurement schemes in the future.

## References:

- [1] P. Schattschneider et al., *Nature Communications* **5**, 4586 (2014).
- [2] G. Ruffato et al., *Physical Review Applied* **15**, 54028 (2021).
- [3] S. Löffler et al., *Quantum* **7**, 1050 (2023).
- [4] P. Schattschneider et al., *Nature* **441**, 486-488 (2006).
- [5] S. Löffler et al., *Ultramicroscopy* **177**, 26-29 (2017).
- [6] S. Löffler, P. Schattschneider, arXiv:2508.01383.

# ATOMIC SCALE INSIGHTS INTO CATALYST DYNAMICS BY ENVIRONMENTAL IN-SITU ELECTRON MICROSCOPY

Marc Heggen<sup>1\*</sup>

<sup>1</sup>Forschungszentrum Jülich GmbH, Ernst Ruska-Centre for Microscopy and Spectroscopy with Electrons, Wilhelm-Johnen Straße, 52425, Jülich, Germany

\*m.heggen@fz-juelich.de

This presentation highlights the importance of environmental in-situ electron microscopy for heterogeneous catalysis, emphasizing its ability to directly visualize atomic-scale structural and compositional dynamics under realistic reaction conditions. Recent microstructural insights obtained using an environmental Hitachi HF 5000 scanning transmission electron microscope are presented for complementary catalyst systems, illustrating the effects of reactive atmospheres, redox conditions, nanoparticle exsolution, and metal–support interactions on nanoscale catalysts.

The first example examines intermetallic ZnPd nanoparticles supported on ZnO during formation (Figure 1) and methanol steam reforming [1,2]. In-situ exposure to methanol-, water-, and hydrogen-containing atmospheres induces pronounced morphological and compositional changes, including nanoparticle faceting and local Zn enrichment. Under reaction conditions, ZnO decomposition and the formation of ZnO surface patches on specific ZnPd facets are directly observed, revealing dynamic restructuring driven by catalytic environments. The second example focuses on PtNi alloy fuel-cell catalyst nanoparticles, demonstrating how reductive hydrogen heat treatment influences structure, activity, and stability for the oxygen reduction reaction. Atomic-scale in-situ observations directly reveal the formation of a thermodynamically stabilized Pt-rich surface skin [3]. Further examples address Ni exsolution in LaNiO<sub>3</sub> and Ni-doped SrTiO<sub>3</sub> perovskites [4,5]. Distinct environment-dependent pathways, including Ni exsolution, migration, oxidation, sintering, Ostwald ripening, and redissolution, are observed employing secondary electron imaging. In Ni-doped SrTiO<sub>3</sub>, two Ni nanoparticle populations with markedly different metal–support interactions and coarsening behavior are identified, providing critical mechanistic insight into the stability limits of exsolution-active catalysts.

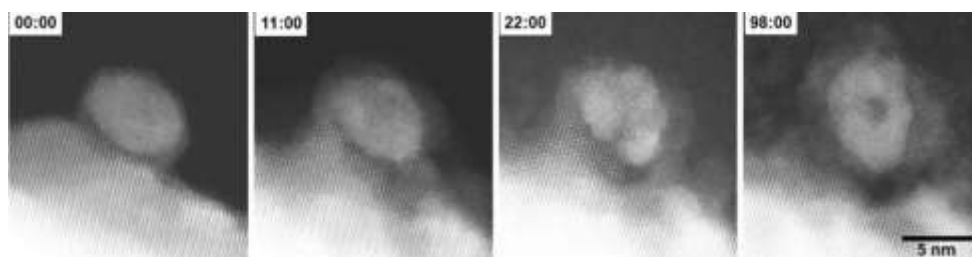


Fig. 1: In-situ DF-STEM image series illustrating reactive metal support interaction and the formation of a ZnPd nanoparticle on ZnO support during reduction in a hydrogen atmosphere (the time in minutes after hydrogen insertion is indicated).

## References:

- [1] A. Meise, M. Heggen, R. E. Dunin-Borkowski, M. Armbrüster, *Small Sci.*, **4**, 2400048 (2024).
- [2] A. Meise, H. Matsumoto, M. Botifoll, R. E. Dunin-Borkowski, M. Armbrüster, M. Heggen, *Small Methods*, in press (2026).
- [3] P. Paciok *et al.*, *Nanoscale* **17**, 25314-25324 (2025).
- [4] P. Cao *et al.*, *J. Phys. Chem. C* **126** (1), 786-796 (2022); P. Cao *et al.*, submitted. (2026).
- [5] D. Jennings *et al.*, *Nat Commun* **16**, 6830 (2025).

# MAPPING OF CRYSTALLINE AND ELECTRONIC PHENOMENA BY ATOMIC RESOLUTION *IN SITU* STEM TECHNIQUES

Alejandra Guedeja-Marron, Francisco Fernandez-Cañizares, Rafael V. Ferreira, Gabriel Sanchez –Santolino, Juan I. Beltran, Lucas Pérez, Maria Varela<sup>1\*</sup>

<sup>1</sup>Universidad Complutense de Madrid, Madrid 28040 Spain.

\*mvarela@ucm.es

Aberration corrected scanning transmission electron microscopy (STEM) combined with electron energy-loss spectroscopy (EELS) and *in situ* capabilities have brought sub-Ångstrom electron beams into visualization and quantification with high accuracy of atomistic phenomena at work. Energy can be transferred into exciting many different degrees of freedom so dynamics, kinetics and other dimensions can be explored at the flick of a switch. This talk will review several examples regarding how high resolution *in situ* STEM techniques (including imaging, spectroscopy or diffraction) can be used to map elusive physical phenomena in functional materials. Examples will include in the first place the mapping of exotic electronic phenomena in nanomaterials for spintronics. Cu nanowires with very low Bi doping levels are very interesting systems due to the giant spin Hall effect reported in bulk, associated with the presence of the high spin orbit coupling Bi species. *In situ* electric current injection through the wires reveals the presence of an orbital Hall effect (OHE) which can be spatially mapped using energy-loss magnetic chiral dichroism (EMCD) spectroscopic techniques. The change of sign in the dichroic signal measured on the nanowire surface upon inversion of electric current exhibits promising fingerprints of OHE derived orbital accumulation within length scales of 2-3 nm. Another example can be found in studies of the magnetic properties of complex oxide ferromagnetic  $\text{La}_{0.7}\text{Sr}_{0.3}\text{MnO}_3$  / insulating  $\text{SrTiO}_3$  interfaces. In these systems, an externally applied electric field may provide a knob to tune the amount of O vacancies at the interface, thus changing the local magnetic properties which can be mapped *in situ*. On a different front, *in situ* 4D-STEM under bias provides the means for atomic resolution characterization of polarization switching phenomena in ferroelectric heterostructures, which may also be affected by local defects. However, noise hampers such measurements, so interpretation relies on a multidisciplinary approach involving advanced characterization, modelling and analysis of the large experimental datasets. Attempts to establish on-the-fly, real time quantification tools that can help with the decision making process on-the-fly will be discussed.

# CORRECTION OF PARTIAL COHERENCE EFFECTS IN PTYCHOGRAPHY

Wouter Van den Broek<sup>1\*</sup>, Holger Kohr<sup>1</sup>

<sup>1</sup>Thermo Fisher Scientific, Advanced Technology, Achtseweg Noord, 5651 GG, Eindhoven, Netherlands

\*wouter.vandenbroek@thermofisher.com

In ptychography, partial coherence effects are commonly accounted for with the so-called mixed-state method, relying on the propagation of 10 to 20 different probes, each to be retrieved along with the object by estimating their respective phase plates. We derived analytical corrections to the coherent diffraction pattern (DP) that follow directly from the incoherent source size and chromatic aberration coefficient, thereby bypassing the need for additional phase plate estimation. It is then straightforward for a derivative-based ptychography algorithm [1,2] to include these terms in the reconstruction process through auto-differentiation. If source size or chromatic aberration coefficient are not known, they can be estimated, and the optimization effort is then reduced to just two extra parameters, resulting in a more robust estimation problem.

The derivation relies on a Taylor expansion of the impinging wavefunction in the probe positions and the defocus, and holds for thick samples. Retaining terms up to second order results in three correction terms for spatial and two for temporal partial coherence. In Figs. 1. and 2., we present results from simulations of a 15 nm thick amorphous alloy, with five slices in the multislice algorithm, an acceleration voltage of 200 kV, a convergence semi-angle of 20 mrad, and an incoherent source size of 15  $\mu\text{m}$ .

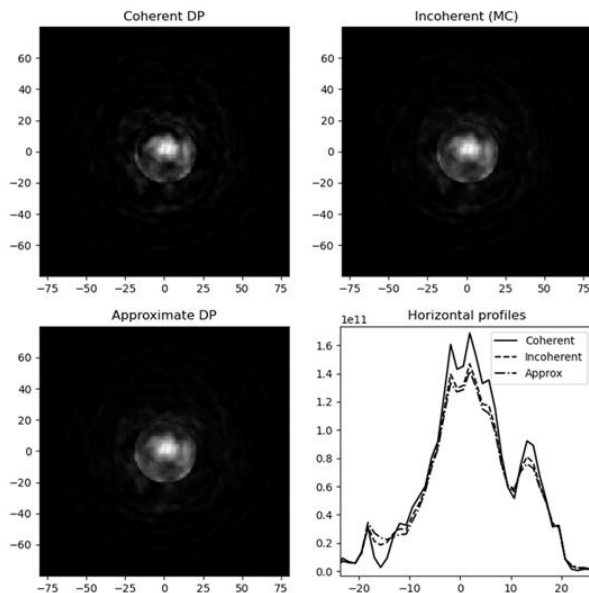


Fig. 1: Our expression (Approx. DP) closely resembles the incoherent DP. The relative errors of Coherent and Approx. w.r.t. the incoherent DP are 26% and 5.9%, resp.

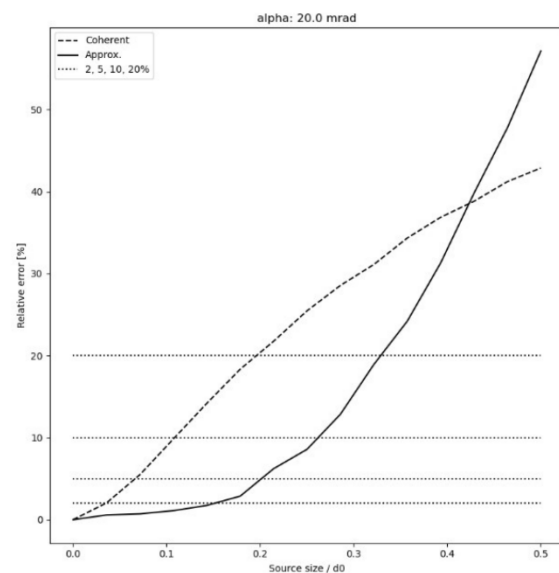


Fig. 2: Relative error w.r.t. the incoherent DP as a function of the incoherent source size relative to the diffraction limited probe size.

## References:

- [1] W. Van den Broek, C.T. Koch, Phys. Rev. Lett. **109**, 245502 (2012).
- [2] W. Van den Broek, C.T. Koch. Phys. Rev. B **87**, 184108 (2013).

# ONGOING STUDIES OF ULTRAWIDE-BANDGAP SEMICONDUCTORS

David J. Smith<sup>1\*</sup>, Ramandeep Mandia<sup>2</sup>, Saurabh Vishwakarma<sup>2</sup>, and Martha R. McCartney<sup>1</sup>

<sup>1</sup>Arizona State University, Department of Physics, Tempe, AZ 85287, USA

<sup>2</sup>Arizona State University, School of Matter, Transport and Energy Engineering, Tempe, AZ 85287, USA

\*david.smith@asu.edu

Ultrawide-bandgap semiconductors (UWBS), such as cubic diamond and boron nitride, and the wurtzitic Al(GaB)N alloys, should be ideal for high temperature and high power electronic devices, especially applications involving high currents and high breakdown fields. However, the fabrication of devices based on these materials remains challenging. Lattice mismatch with viable substrates invariably results in interfacial misfit dislocations and threading defects during epitaxial growth. Moreover, controlled doping, essential for device applications, is difficult to achieve. This talk will describe some of our recent collaborative studies of UWBS materials and heterostructures where electron microscopy techniques played a valuable role in enabling significant progress to be made in resolving these critical growth issues.

Cubic boron nitride ( $a_0 = 0.3615\text{nm}$ ) and cubic diamond ( $a_0 = 0.3567\text{nm}$ ) are closely lattice-mismatched, but the ready formation of BN allotropes, especially the  $sp^2$ -bonded rhombohedral (*r*-BN), hexagonal (*h*-BN) and turbostratic (*t*-BN) phases, proved to be a persistent problem in the growth of c-BN/diamond heterostructures until optimal growth conditions were established [1, 2]. The differences in phase and interfacial structure across BN/diamond heterointerfaces was shown to cause a threefold difference in interfacial thermal conductance, which could prove to be a key factor in practical applications requiring heat dissipation at high current densities [3]. Ultrathin barrier AlBN/GaN high electron mobility transistors with highly promising device performance were fabricated [4], but attempts to grow thicker AlBN layers on nitrided sapphire substrates with B concentrations as high as 15% resulted in considerable degradation of structural quality [5]. Other examples to be described include epitaxial c-BN films grown on nitrogen-plasma-terminated B-doped diamond where a dramatic shift in the conduction band offset between the two materials was measured [6]. 'Lossless' phonon transitions through GaN-diamond and Si-diamond interfaces were achieved using thin interlayers of amorphous silicon dioxide and amorphous SiC [7].

Acknowledgments: This work has been supported by ULTRA, an Energy Frontiers Research Center funded by the US Department of Energy Office of Science Basic Energy Sciences under Award DE-SC00211230 (P.I. R.J.Nemanich). Ongoing collaborations with the groups of Robert Nemanich, Houqiang Fu and Nidhin Kalarickel (ASU), Srabanti Chowdhury (Stanford), Richard Wilson (UC-Riverside), Debdeep Jena and Grace Xing (Cornell), and Martin Kuball (Bristol) are also gratefully acknowledged.

## References:

- [1] A. Patel, *et al.*, APL Materials **13**, 061104 (2026).
- [2] S. Vishwakarma, *et al.*, J. Appl. Phys. **137**, 155302 (2025).
- [3] S. Khan, *et al.*, APL Materials **14**, 021107 (2026).
- [4] C. Savant, *et al.*, Appl. Phys. Lett. **126**, 112906 (2025)
- [5] C. Savant, *et al.* J. Appl. Phys. **139**, 063101 (2026).
- [6] A. Yekta, *et al.*, Appl. Phys. Lett. **127**, 171603 (2025).
- [7] M. Malakoutian, *et al.*, Adv. Electronic Maters. 2400146 (2024).